Preferred citation: D.S. Keller, D. Branca and O. Kwon. Spatial partitioning of the structural properties of tissue and towel grades. In **Advances in Pulp and Paper Research, Oxford 2009**, *Trans. of the XIVth Fund. Res. Symp. Oxford, 2009*, (S.J. I'Anson, ed.), pp 693–719, FRC, Manchester, 2018. DOI: 10.15376/frc.2009.2.693.

SPATIAL PARTITIONING OF THE STRUCTURAL PROPERTIES OF TISSUE AND TOWEL GRADES

D. S. Keller[1, 2], D. Branca[2] and O. Kwon[2]

[1]Department of Paper and Chemical Engineering, Miami University, Oxford, OH USA, 45056

[2]Faculty of Paper Science and Engineering, SUNY College of Environmental Science and Forestry, Syracuse, New York USA, 13210

ABSTRACT

This paper describes an investigation conducted to examine the mesoscale structural properties of single-ply tissue and towel papers by mapping thickness, out-of-plane deformation, formation, and density. The uniformity of each of these properties was studied to a zone size of 0.1 mm in mapped regions of about 10 mm square. The sampling regions were partitioned into subsets that were separately analyzed. Regions of interest included wet pressing marks, embossed patterns and through air drying (TAD) pressed patterns. The relationship between thickness and grammage (basis weight) in the different regions of interest were compared. Differences were attributed to the indentation process that could affect the structure in different ways, depending on the process conditions. Six commercial tissue and towel products were tested.

The regional differences were most apparent in the results for paper towels. Deformation of the structure to form textured patterns compressed regions and increased the local density. There was selected in-plane movement of fibers, in response to the indentation. The towel sample formed by wet pressing did not show the same extent of densification at the indentation site. The structure was deformed out of plane, but not significantly compressed. Tissue samples formed by conventional wet pressing showed increased densification at points of indentation. Differences in the out-of-plane response to the pressing process could be distinguished between different tissue samples.

INTRODUCTION

From the most casual perspective, printing papers and tissue papers have very few similarities as web structured materials other than the fibers they are composed of. Papers used as imaging media have a long list of important attributes, such as the need for a flat planar surface of uniform smoothness so that inks are distributed evenly and remain at the surface. Papers need to be strong enough to be drawn through a web printing process, or have sufficient flexural stiffness to run the path of a sheet fed imaging process without jamming or misfeeding. The structural evenness is also important for uniform light reflectance so that whiteness, opacity and look through formation are aesthetically acceptable. On the other hand, tissue and towel grades have material requirements that are almost diametrically opposed to those of printing grades. The need for absorptivity, durability and softness to the touch suggests a much more porous structure that allows fibers to more freely interact with fluids, especially water. The paper web may be disrupted by creping or embossing to open the structure and provided additional specific surface area. The extent of bonding is much lower and the distribution of z-fiber orientation is much broader, accomplished either by induced deformation that results in a more felt-like structure. Ramasubramanian provided a comprehensive review of the properties of tissues and towels, with a special focus on the influence of creping on the web structure [1]. Basis weights for a single ply of towel and tissue are generally lower than printing papers. However, there is an overlap of grammage between newsprint and paper towel grades, even though there are stark differences in the material characteristics. All of our senses, standard tests and experiences suggest that these are vastly different web structures.

Considering of all of the potential differences, printing grades and tissue/towel grades have at least one common property that is of critical importance in meeting their end use performance; that is their in-plane tensile strength. However, for these two grades, the development of dry strength in the web must be approached differently. To achieve softness and flexibility, tissue and towels require an overall lower degree of bonding (whether by mechanical or chemical bond disruption). To fortify strength, a deterministic pattern of densified regions is introduced to form a reinforcing network of much larger length scales, on the order of 10^{-3} m, that softwood fibers can span to provide strength. Printing grades have much more uniform level of densification of closely spaced interfiber bonds along the length of the fiber that impart strength and stiffness in the web at length scales of about 10^{-5} m.

Printing papers rely on a high level of bonding and webs with relatively high density (low porosity). The restrained shrinkage of fibers at micrometer lengths induces internal stresses that contribute to in-plane tensile strength, stiffness and rattle. Free fiber lengths and characteristic dimensions of interfiber bonds are on the order of 10^{-5} m and the strain potential brought on in the drying process occurs within the bonds and cell wall at dimensions less than 10^{-6} m. Longer softwood fibers provide the continuous reinforcing network to meet tensile strength requirements. Hardwood fibers and fillers further contribute to space filling, contact points and bonding as they increase web uniformity.

Strength development in tissue and towel grades is similar to that of printing grades, although it is done at much larger length dimensions and with a much greater amount of systematic intervention. Rather than focusing solely on the millimeter length reinforcing elements and the interfiber bonds that connect them, tissues and towels use pressed regions in organized patterns to form a reinforcing network of sufficient strength to meet product requirements. Pattern design and web densification are controlled to manage tensile strength and a number of other properties. Liang and Suhling [2] modeled embossing using finite element analysis and demonstrated the differences in densification and strain in the web that results from different pressures and backing materials. By leaving the unpressed regions in a less bonded state, the bulk and conformability of the entire web is increased. Further bulking of the web can occur as a result of creping the structure or by disrupting interfiber bonds with chemicals or in the air drying processes. So in fact, a critical consideration of the web properties of tissues and towels occurs at the mesoscale region, between 10^{-2} and 10^{-4} m. The cell wall structure and interfiber bonding still remain important elements in web strength.

The objective of this investigation was to examine the structural properties of tissues and towels in length scales spanning from larger than fiber widths (50μm) into the dimensions of paper testing (< 100 mm). One specific goal was to collect data matrices for the structural properties of tissue and towel samples at a sampling size and resolution so that the variability of these properties could be quantified and analyzed. The approach was to apply existing formation and thickness mapping methods to obtain density maps.

Since tissue and towel samples have distinguishable regions where these properties will differ, this study explored the ability to partition, or deconvolve these properties to provide a more detailed characterization of the structures. The study will test the hypothesis that regions deformed by press drying or embossing will not necessarily be densified in the process. The study also seeks to quantify the fibrous movement at the embossing site, and whether grammage loss accompanies the indentation process.

MATERIALS AND METHODS

Materials

Commercially available tissue and towel products were examined in this study. Single ply samples were arbitrarily selected as representative of common grades of paper towel, napkin and bathroom tissue. Table 1 identifies the samples and provides the values for grammage and flat platen thickness measured by TAPPI standard methods T410 [3] and T411 [4].

Incident light photographs of the towel samples are shown in Figure 1, and the napkin and tissue samples in Figure 2. The regular pattern of induced deformation from wet pressing or from the creping process may be observed in several of the samples. The non-uniform distribution of fibers from the formation process can also be seen in these images.

Figure 3 shows SEM micrographs of some of the induced features in these samples. The figure shows the pressed features from PT3, N1 and TP1, and the creped pattern created in TP2. Considering once again the photographs in Figure 1 and Figure 2, an irregular pattern of surface roughness generated by the stochastic distribution of fibers and cockling may also be seen in several of the samples.

Table 1. Identification of tissue and towel samples with TAPPI Std values for grammage and thickness.

Sample		*Manf.*	*Grammage (g/m^2)*	*TAPPI Std. Caliper (μm)*
PT1	Paper Towel	PG	38.8	210
PT2	Paper Towel	Ind.	34.0	132
PT3	Paper Towel	KC	38.6	181
N1	Napkin	GP	16.5	58
BT1	Bathroom Tissue	GF	20.3	98
BT2	Bathroom Tissue	KC	18.0	88

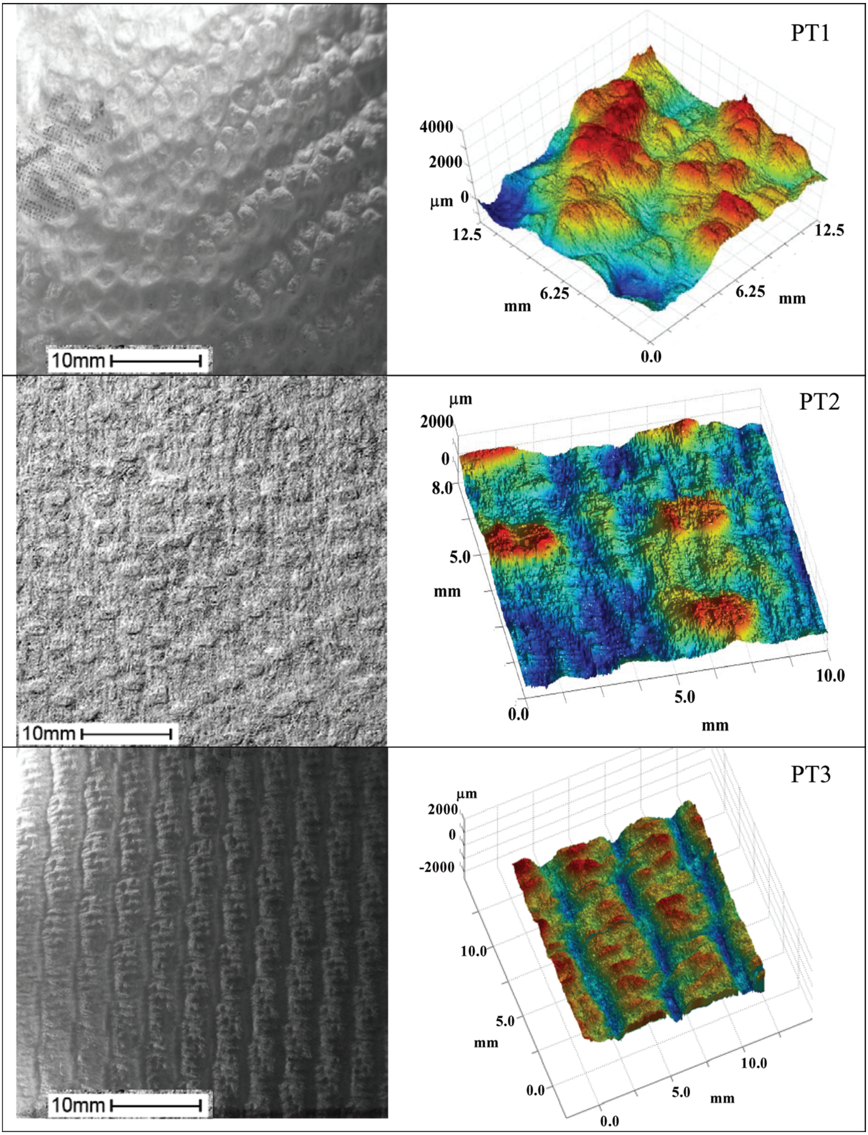

Figure 1. Images of the paper towel samples, PT1, PT2 and PT3. Incident light photographs are shown in the left column. The right column shows perspective views of the out of plane deformation as determined using twin laser profilometry, discussed in detail below.

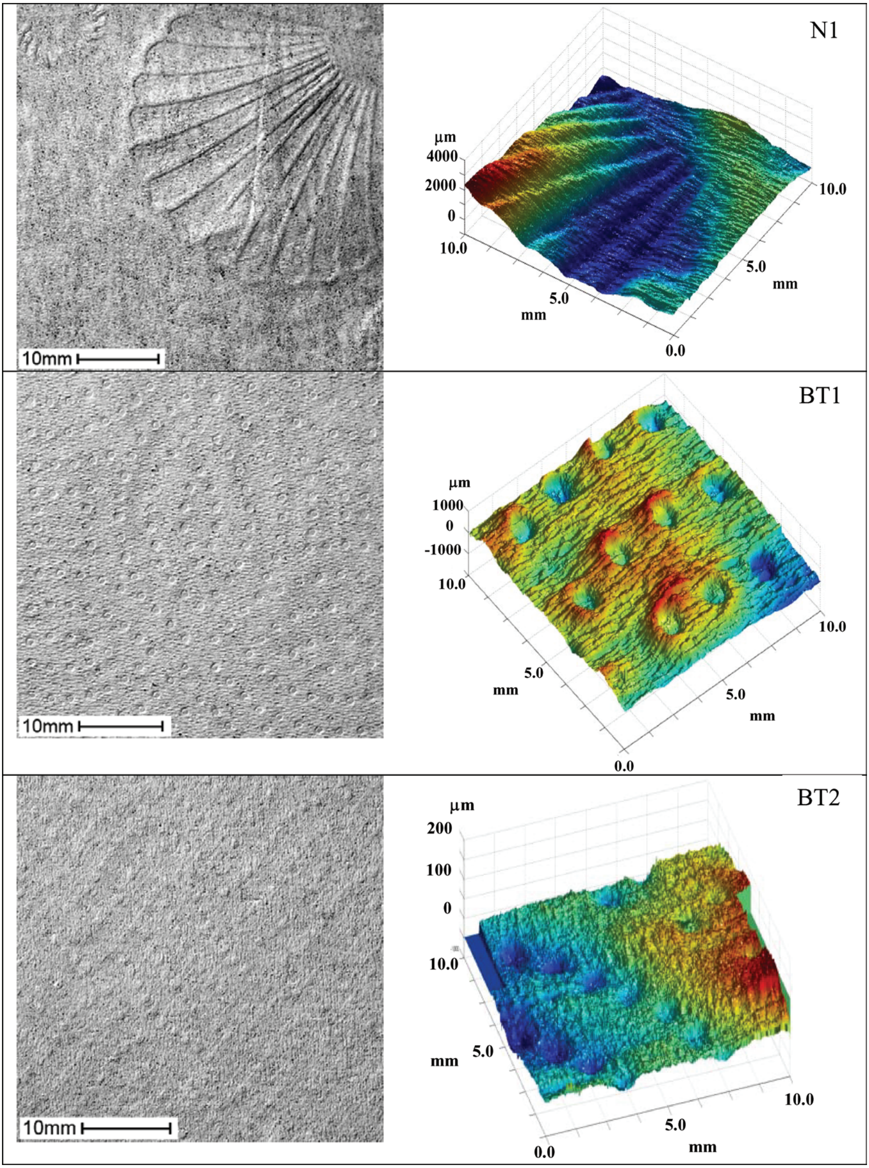

Figure 2. Images of the napkin and bathroom tissue samples, N1, BT1 and BT2. Incident light photographs are shown in the left column. The right column shows perspective views of the out of plane deformation as determined using twin laser profilometry, discussed in detail below.

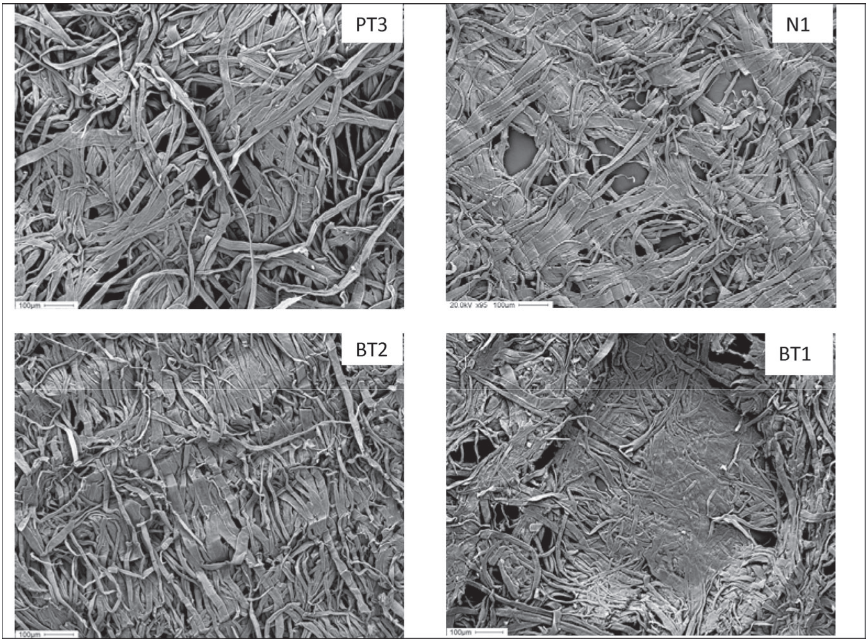

Figure 3. SEM micrograph images of tissue and towel samples: PT3 (top left), pressed indentation; N1 (top right), shell pressed pattern; BT2 (lower left) creped structure; BT1 (lower right) pressed indentation.

Test specimens were prepared by cutting to 70mm × 70 mm in order to fit the profilometer sample frame. To test the optical reflectivity of samples, regions were sputter coated with Gold-Palladium (Au-Pd) on the front and back side. A Mylar mask was used to create a 10 mm × 10 mm square region in one corner of each sample that was coated using a Denton Desk II (Denton Vacuum USA). This treatment was previously shown to render the fibers fully reflective, without disrupting the fibrous structure [5]. By comparing coated and uncoated regions, the accuracy of optical profile measurements was verified. For several samples, a small (~1 mm) square of reflective tape was placed at the corner of the sputter coated region for use as a registration mark to align topography maps with grammage maps for further analysis. For samples PT1 and PT2, perforations were made in four corners of the scanned region in order to allow registration of maps in both translation and rotation.

Samples were conditioned according to TAPPI standard method T402 [6] before all formation or thickness tests. A saturated salt bath of calcium nitrate was used to maintain a constant humidity of 52% at 22°C in the profilometer test chamber.

Paper formation imaging

β-radiographic transmission imaging was used to obtain the local grammage maps (paper formation) of the samples. The method is described in detail by Keller and Pawlak [7,8]. The radiation source was a ^{14}C polymethyl methacrylate plate (20mm × 25mm × 1mm) (Amersham Co.). Samples were placed between the source and the phosphor imaging screen (Model S0230, Eastman Kodak). Screens were exposed for 45–60 min, after which the screen containing the latent image placed in the storage phosphor imager. The image was digitized using a Molecular Dynamics Phosphor Imager SI (Sunnyvale, CA) at a spatial resolution of 100 μm. The data matrix generated by the scanning process was converted into grammage maps using a calibration constant determined from Mylar films of known grammage. A precision of ~0.1 g/m^2 is obtained using this method.

Topographical maps

The two sides of paper samples were scanned simultaneously to obtain topographical maps using the Twin Laser Profilometer (TLP). A complete description of the design and operation of this instrument was provided in an earlier work by Sung *et al.* [5,9]. The instrument, pictured in Figure 4, may be considered in three main parts: the laser range sensing systems, the sample frame, and the main (X-Y) positioning units.

Two high precision laser range sensors (DRS 300 (Cyber Optics Corp., Minneapolis, MN), were used to detect the distance from the sensor to the surface along the Z-axis, normal to the sample surface. The range sensors use triangulation of the focused 670nm laser beam to detect distance to a reproducible resolution of 1 um. The beam produces a 10–20 μm diameter spot on the surface of the sample which is reflected back to the detection optics and a CCD detector. In theory, the reflected light forms a normal distribution of intensity in the detector array, of which the position is a function of the distance to the reflecting surface. For the rough surfaces of the samples tested in this investigation, the actual spot formed in the detector array was at times irregular or discontinuous. In all cases, the centroid of the detected intensity for the top 2/3 of the peak was used to resolve the distance to the surface. The full scale detection range of each sensor is 300 μm. To expand the operating range of the instrument, each sensor was affixed to a Z-direction positioning stage with a 100 mm positioning limit and a resolution of 0.5 μm. Once

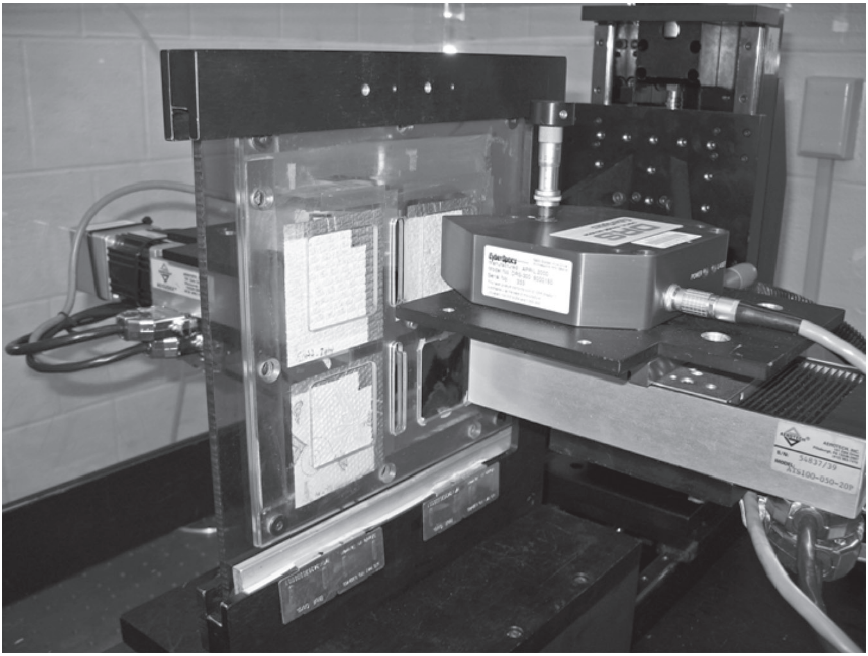

Figure 4. Photograph of the Twin Laser Profilometer (TLP). The sample frame holds the samples vertically between the laser range sensors. Laser range sensor shown in the foreground is affixed to a Z-positioning stage that moves the sensor to keep it within the operating range. The micrometer on top of the sensor is used to vertically align the reflected spot position. The Y-positioning stage is visible to the right in the background.

calibrated in space, the combination of any stage movement and the output from the laser range sensor was used to determine the Z-direction position to a resolution of 1 μm. In the event that the range detected by the sensor exceeded a specified limit, the Z-positioning stage was incremented, and the sensor samples the range once again. If a discontinuity, such as a large step or void was encountered, the control systems entered a seek mode to locate the surface if at all possible. If it could not be found, the instrument considered this a "dead spot", and the point was excluded from the working data set.

The simultaneous topographical mapping of both surfaces was made possible by using two laser range sensing systems held in opposition along the Z-axis, as shown in Figure 4. A support bracket fixes the separation distance between the two Z-positioning stages and coordinated movement in the X-Y direction. The separation of the Z-range sensing systems was calibrated using a 57 μm tungsten foil thickness standard. This provided an accurate determination of thickness as the separation distance between the two surfaces. The in-plane position of measurement spots from the two range sensing systems were aligned using horizontal and vertical edges of square opening etched into the thickness standard. Alignment to within ± 3 μm was possible using micropositioners. To avoid interference between the laser sensors, only one side is sampled at a time. The sampling rate of each sensor ranged from 0.2 to 1 Hz and was primarily slowed by surface discontinuities such as voids or steps that exceeded the sensor range.

The sample frame was used to hold up to four samples vertically between the opposing range sensors, cf. Figure 4. The exposed region of each sample was 50 mm × 50 mm. The X and Y positioning stages were used to move the Z-support bracket in order to map topographies. A square region of up to 130 mm can be mapped in the X and Y directions to a resolution 1 μm. In this study, scans were typically performed on the 12.5 mm or smaller region near the center of the exposed region. Thickness maps were developed by collecting a line scan in the X-direction and then incrementing to the next line in the Y-direction. The step increment in both directions was 25um.

Thickness and out-of-plane deformation maps

Sung *et al.* [5,9] introduced the approach used to obtain thickness and out-of-plane deformation (OPD) maps from the two topographical maps as shown in Figure 5. Thickness at each in-plane position was determined by taking the pointwise differences between the two topographical maps. Out-of-plane deformation is defined in this work as the net Z-displacement of both topographical surfaces with regard to the original Z-positions of the two surfaces. By taking the pointwise average between the surfaces, an imaginary center plane that bisects the bulk phase is determined, as illustrated in Figure 5.

Density maps

Density refers to the mass per unit volume of a material including void spaces. It may also be calculated by dividing the grammage by the thickness. However, for fibrous web structures, the true intrinsic density is not strictly defined, since the externally boundary surfaces used to measure thickness are a function of the measurement method or model. By reducing the zone size of thickness measurement, the average density for many measurements increases to approach the intrinsic density [10]. For the twin laser profilometer, the surface is defined as the average reflected distance within a 10um spot projected onto the surface. It was previously demonstrated that the

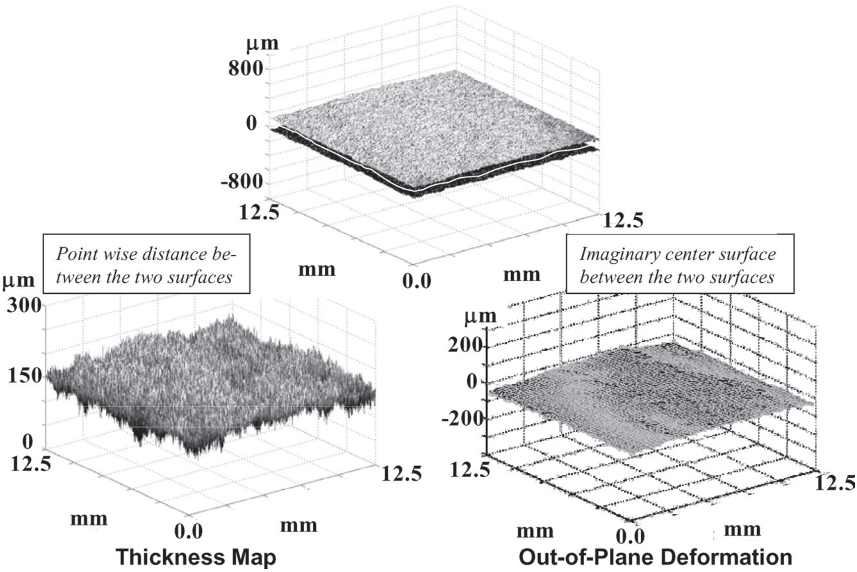

Figure 5. Method for mapping local structural parameters using aligned top and bottom surface topographical maps. The pointwise separation distance between the two maps yields a matrix representing the local thickness. The imaginary surface that bisects the space between the top and bottom surfaces represents the out-of-plane deformation (OPD). Reprinted from Sung *et al.* [5].

non-contact thickness measurement obtained using the TLP method closely approximates the intrinsic density [5,11]. Since the resolution of the grammage maps (100 μm) differs from the thickness maps (25 μm), the latter needed to be dilated to 100 μm using a local averaging function. The two data sets could then be aligned using registration marks and maximization of two dimensional correlation coefficients. Local density maps were obtained by the pointwise reduction of grammage values by thickness values.

Spatial partitioning of structural maps was performed by applying a masking matrix to select specific regions of interest. In this study, the ROI mask was generated by selecting regions based on thickness in order to focus on the patterns formed by wet press patterns. By applying a binary threshold of thickness around a specific region, the imprint of the pressed region was marked. Further analysis was conducted on the partitions isolated by this process.

RESULTS

Structural maps

The results for mapping the thickness, out-of-plane deformation, formation and density for each sample are illustrated in Figure 6-Figure 11. In all figures, the machine direction is parallel to the vertical axis. Discussion in this section will be limited to the qualitative interpretation of the various maps, and how differences between samples may be identified by inspection of structural maps.

The top two panels in Figure 6 show the results obtained from profilometic measurements using the TLP instrument for paper towel sample PT1. The pattern induced by the through air drying (TAD) step is evident in both OPD and thickness maps. Local cockle or curl deformation within the sample may be seen in larger regions of displacement, such as the lower left corner as

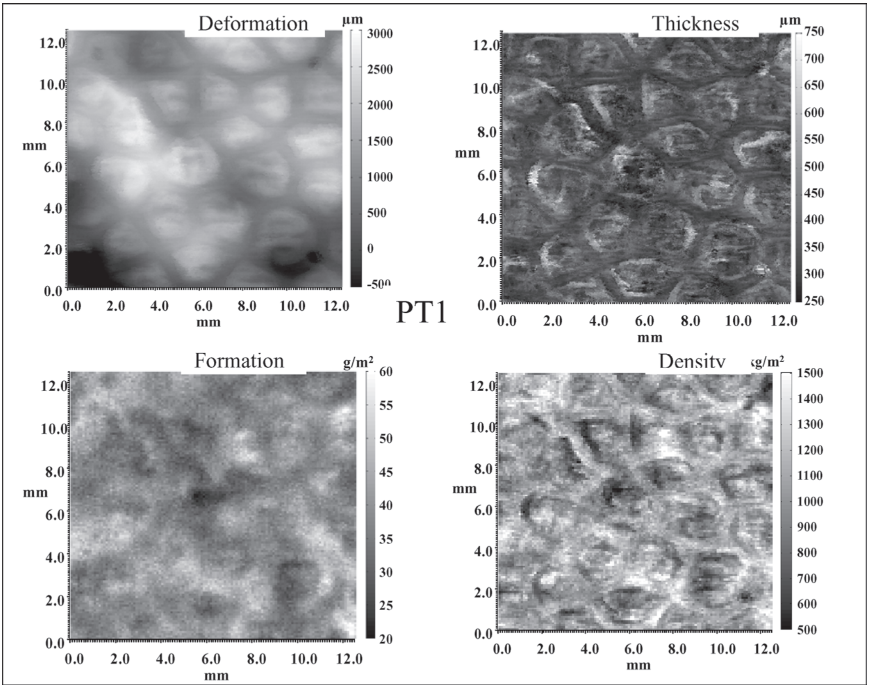

Figure 6. Structural maps for sample PT1. Out-of-plane deformation (top left) and Thickness (top right) are plotted at a resolution of 25 µm. The grammage map, or formation (lower left) and local density (lower right) are plotted at a resolution of 100 µm.

compared to the left center region. The variation in OPD is more clearly presented in the color plates of the OPD shown in perspective in Figure 2. It is evident that OPD is a dominant feature of this structure by comparing calculated maps with the incident light photographs in the same figure. Inspection of the thickness map, cf. Figure 6, shows considerable thinning of the structure along the margins between the embossed features. Thicker regions are detected at the edge of the features, which are likely artifacts resulting from measuring the Z-direction thickness of the vertical wall at the abrupt displacement of the structure.

The local grammage map for PT1, provided in the third panel of Figure 6, show the redistribution of mass due to the patterning process. There is good correlation between the regular features seen in the thickness and grammage maps. The stochastic flocked structure of fibers also correlates well between these two structures. For example, there appears to be a lightweight zone located at 7 mm (V)ertical /6 mm (H)orizontal which appears as a thin spot in the thickness map. Other flocked regions that correspond to thicker regions may be found randomly distributed within the structure.

Now consider the second paper towel sample, PT2, as shown in Figure 7. The oval features seen in the deformation map are the result of the wet pressing process and are seen more clearly in the color plates in Figure 2. Notice the there is little or no evidence of these features in either the thickness or formation maps. This suggests that the indentation process neither densified the region, nor redistributed the mass. Stochastic regions of high and low mass that appear to be the result of the forming process or where the structure has fractured correlate well between the thickness and formation maps. The calculated density shows how regions of high grammage and thickness, cf. 4–7 mm V / 1 mm H, have densities that are close to the average. However, an apparent fracture zone at 6 mm V / 6–9 mm H shows a region of very low density.

The third Paper towel sample, PT3, shows two distinct features in the deformation and thickness maps shown in Figure 8, and the color plate in Figure 2. The vertical bar pattern is the result of the wet pressing pattern. Closer inspection also reveals a creping pattern parallel to the horizontal axis. There appears to be thinning of the structure along the peak of the bar pattern. Once again there appears to be a thicker region along the border of the pressed regions that may result from the abrupt discontinuity of the structure. The creped structure is visible in both the deformation and thickness maps. This suggests that the structure is undergoing significant pleating and bulking during the creping process.

The embossed decorative pattern of a napkin paper may be observed in

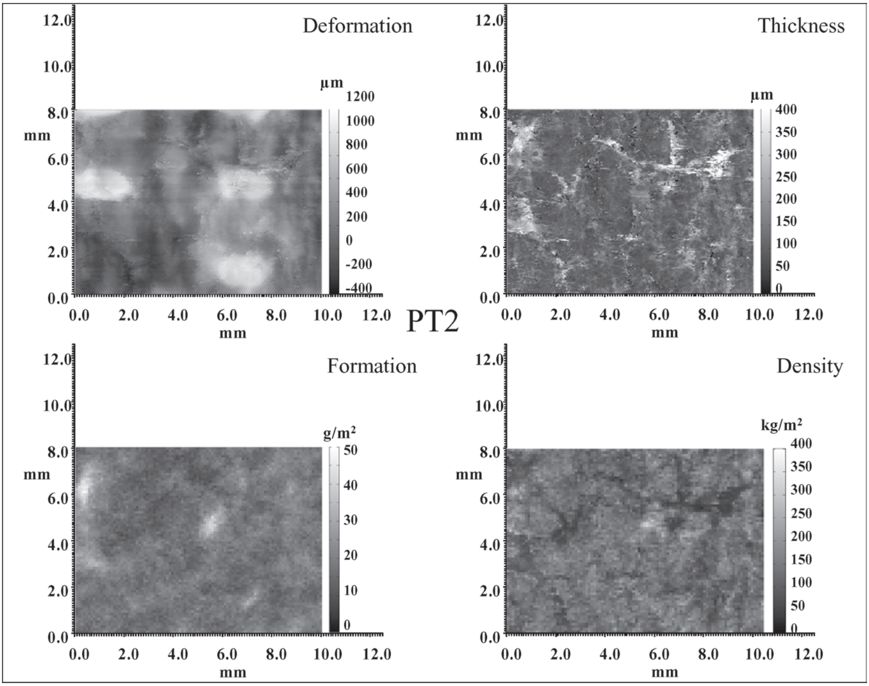

Figure 7. Structural maps for sample PT2. Out-of-plane deformation (top left) and Thickness (top right) are plotted at a resolution of 25 µm. The grammage map, or formation (lower left) and local density (lower right) are plotted at a resolution of 100 µm.

the structural maps, cf. Figure 9, and in the color plates of Figure 2. The patterning process causes both out-of-plane deformation and compression and bulking of the structure. No redistribution of is evident in the formation image. This results in a considerably wide range of densities in the pressed region. The structure is strengthened with this pattern, while adjacent regions are low density for enhanced absorbency.

The structural maps for two samples of one-ply bathroom tissues, BT1 and BT2 are provided in Figure 10 and Figure 11. While the two samples have similar features, such as a regular pattern of wet pressing indentations and a distinct creping pattern that is visible in both the deformation and thickness maps, there are also subtle differences between these products that could shed insight into the paper performance. For instance, the embossed wet press pattern for BT1 deforms in the opposite direction around the perimeter, cf.

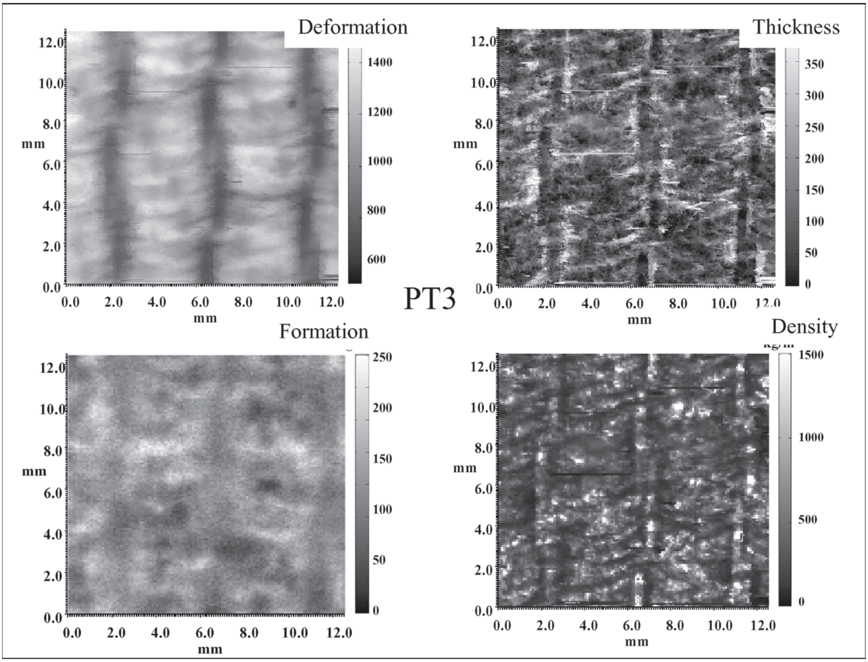

Figure 8. Structural maps for sample PT3. Out-of-plane deformation (top left) and Thickness (top right) are plotted at a resolution of 25 μm. The grammage map, or formation (lower left) and local density (lower right) are plotted at a resolution of 100 μm.

Figure 10 and especially Figure 2. BT2 on the other hand, does not exhibit a similar reversed deformation.

ANALYSIS AND DISCUSSION

Spatial partitioning

The structure of tissue and towel products has a much more systematic and complexly engineered structure as compared to communication papers. Isolating specific regions for separate analysis is a useful approach towards determining how specific processes influence the web structure, and how the differences in structure affect the final bulk properties. The first approach performed in this study was to analyze the structural properties as spatially partitioned between the pressed and unpressed regions. Three samples, PT1,

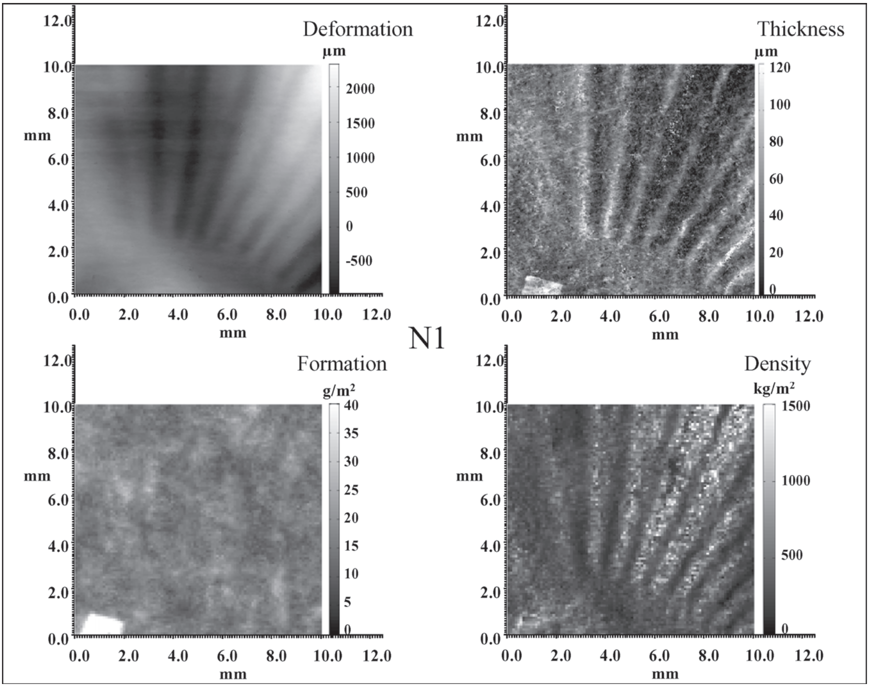

Figure 9. Structural maps for sample N1. Out-of-plane deformation (top left) and Thickness (top right) are plotted at a resolution of 25 µm. The grammage map, or formation (lower left) and local density (lower right) are plotted at a resolution of 100 µm.

PT2, N1 and BT1 were partitioned using the pressed thickness region to form a partitioning mask, shown in Figure 12.

The mask for sample PT1, cf. Figure 12, was formed by tracing the pressed region of interest (black) and unpressed regions (white). Figure 13 shows a scatter plot of the values for thickness plotted as a function of grammage for points falling in the two partitioned regions of interest. The contour line marks a level of constant population and distinguishes between the thinner pressed region and the unpressed region that shows a broader distribution of thickness. The symbols mark the mean values for the distribution along both axes, the values of which are provided in Table 2. As one would expect, there is significant difference between the thickness values in the two regions. Also, drying does not disturb the subtle relationship between thickness and grammage evident as the slight positive slope of the distributions. One would

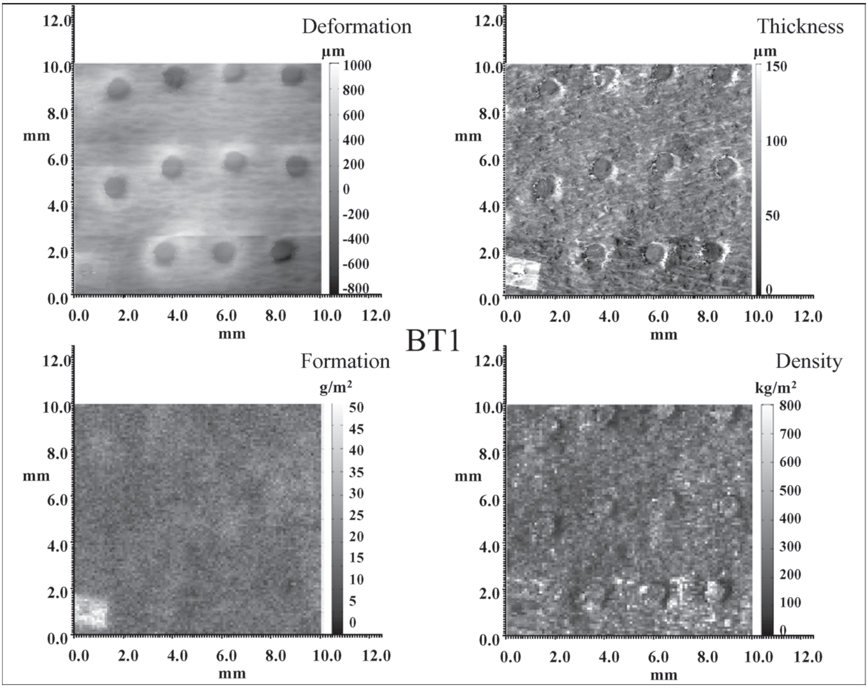

Figure 10. Structural maps for sample BT1. Out-of-plane deformation (top left) and Thickness (top right) are plotted at a resolution of 25 μm. The grammage map, or formation (lower left) and local density (lower right) are plotted at a resolution of 100 μm.

Table 2. Peak maximum values for thickness vs. grammage distributions for the spatially partitioned regions.

	Pressed Region			*Unpressed Region*		
Sample	*Masked %*	*Thickness (μm)*	*Grammage (g/m²)*	*Masked %*	Thickness *(μm)*	*Grammage (g/m²)*
PT1	38.1	341	38.9	61.9	380	39.1
PT3	11.9	106	18.7	88.1	123	18.6
N1	35.7	47.5	16.1	64.3	31	17.3
BT1	7.7	61.4	17.5	92.3	63.0	18.3

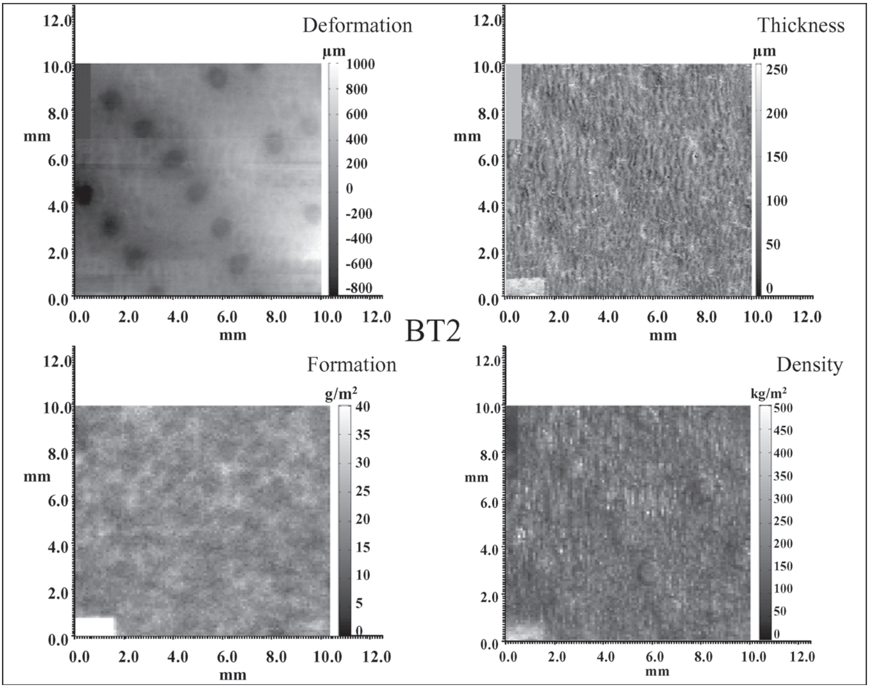

Figure 11. Structural maps for sample BT2. Out-of-plane deformation (top left) and Thickness (top right) are plotted at a resolution of 25 μm. The grammage map, or formation (lower left) and local density (lower right) are plotted at a resolution of 100 μm.

expect that the marking pattern does not preferentially compress high grammage regions, since it is a fixed pattern of marking (unlike hard nip calendaring [5]). The difference between mean values for grammage in the pressed and unpressed regions is insignificant. This suggests that in-plane movement of material is minimal when features are formed in the TAD process.

We therefore focused on the thickness values observed for sample PT1, plotted in Figure 14. The solid black line shows the experimentally determined probability distribution of thickness for the sample. It was found that this distribution could be accurately modeled by applying normal distributions of the partitioned regions by using the mean values and relative proportions listed in

Table 2. The result is plotted as a dashed line in Figure 14. The small

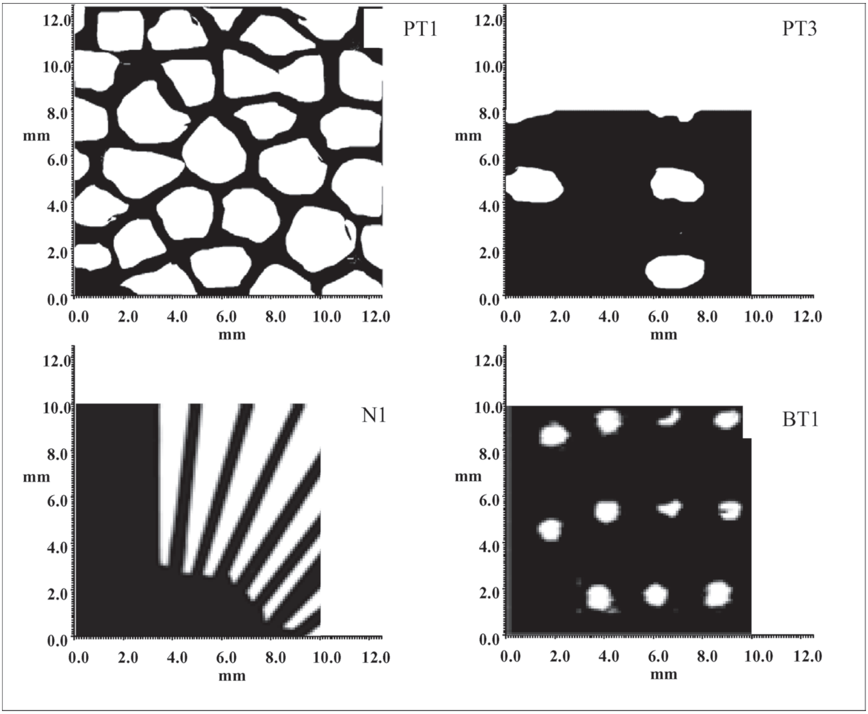

Figure 12. Image masks used to partition pressed and unpressed regions. Sample PT1 (top left), PT3 (top right), N1 (lower left), BT1 (lower right).

amount of residual difference between the model and experimental that occurs from 450–650 um was found to be the narrow regions that occur at the crest of the unpressed region. These are either high grammage sites, where fiber have been displaced to the top of the embossed feature, or vertical walls that give are interpreted by the instrument regions of high thickness. The residual represents only a small fraction (<10%) of the thickness values in the sample.

A second paper towel sample was analyzed in the same manner as PT1. Figure 15 shows thickness plotted as a function of grammage for PT2 after partitioning with the mask shown in Figure 12. In this instance, the regions were not selected based on a difference in thickness. The mask was generated by thresholding the OPD map to select the circular features that protruded out-of-plane, as seen in the OPD map in Figure 7 and Figure 1. Although the pressed region (confined by the black contour line) represented about 12% of

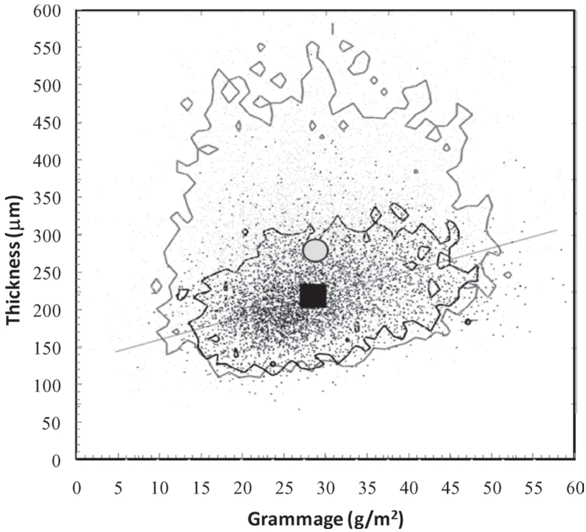

Figure 13. Distribution of thickness vs. grammage for sample PT1. Contour lines indicate equal levels of constant population for the unpressed region (gray) extending to higher thickness values, and the pressed region (black) confined to lower thickness values. The symbols mark the mean values of the distributions; circle – unpressed, square – pressed. The regression line for the pressed region is shown on the figure, where a direct relationship between thickness and grammage exists.

the overall area, it is evident that the indenting process caused significant planar deformation with little densification of the web. One would expect that there would be little gain in strength since pressing features do not appear to increase bonded area. Figure 15 also shows that inplane movement of fibers around the features is minimal, based on the similarity of the grammage distributions.

Thickness was used as the spatial partitioning criterion for sample N1, the napkin sample with a decorative embossed pattern. From the structural images, cf. Figure 9, both web densification and out-of-plane deformation occur during the indentation process. A web mask was created by manually outlining the embossed features on the thickness image and is shown in Figure 12. The plot of thickness vs. grammage is shown in Figure 16. The pressed region is indicated by the black contour line at significantly lower thickness values. The peak maxima for thickness and grammage are provided in Table 2. The median values for the pressed and unpressed distributions are marked by the symbols in the figure. The embossing process reduces thickness

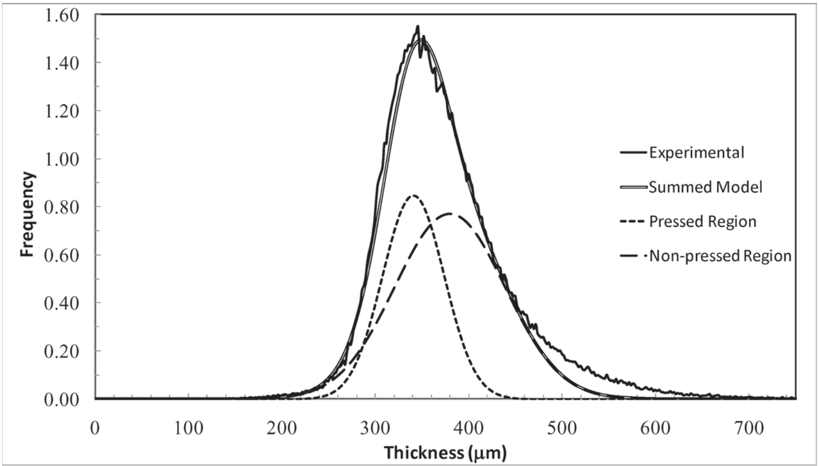

Figure 14. Frequency distribution of thickness values for sample PT1. The experimental data is shown as the solid line. Two normal distributions were generated from the statistics of the distributions measured inside and outside of the mask, i.e. the non-pressed and pressed regions. The area under the curve represents the spatial coverage for each of the two partitions. The distributions are centered and the mode. The pressed region is shown as a fine dashed line and the unpressed region shown as a coarse dashed line. The sum of the two model distributions is shown as the double line.

and also appears to displace some of the fibrous material from the pressed region as indicated by the decrease in mean grammage. The distribution of thickness for sample N1 is illustrated in Figure 17. Once again, the experimental distribution can be represented as the sum of weighted normal distributions generated from the peak maxima from the partitioned regions. The residual that occurs at thickness greater than 60μm can be seen to occur along the edge of the embossed features.

The tissue sample BT1 was partitioned based on thickness values in pressed regions, and the resulting distributions were analyzed. Figure 18 displays the contour maps for the pressed and unpressed regions. The OPD map shown in Figure 10 was used to generate the image mask shown in Figure 12. By applying a regional threshold, the flat region at the apex of the pressing feature was selected. Since the pressed region comprised less than 10% of image, individual points were omitted from Figure 18 to enable the two distributions to be compared. It can be seen that there is little difference between the mean grammage values or thickness values for the pressed and unpressed

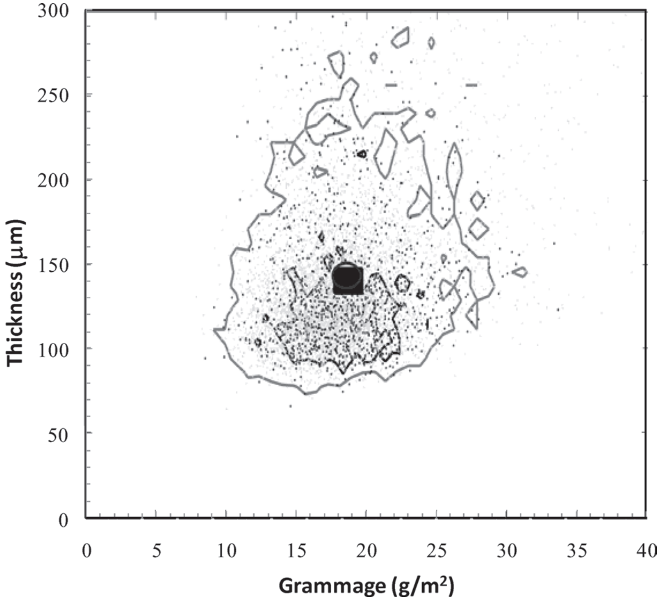

Figure 15. Distribution of thickness vs. grammage for sample PT2. Contour lines indicate equal levels of constant population for the unpressed region (gray) extending to higher thickness values, and the pressed region (black) confined to lower thickness values. The symbols that mark the mean value of the distributions are superimposed.

regions. Figure 19 show that by modeling the thickness values in the two regions with normal distributions, the weight sum can closely approximate the observed distribution. This suggests that for the low grammage samples such as tissues, the differences of local structural properties between the pressed and unpressed regions are small and more difficult to quantify with confidence.

CONCLUSIONS

The focus of this investigation was on the tissue and towel paper grades that typically contain multiple regions where the structure has been intentionally changed from a simple deposition of fibers seen in denser papers. The spatial nonuniformity exists, not only as the result of the forming process, but also as a result of deformation in thickness and planarity. The laser based optical method described in this study was found to be well suited for mapping

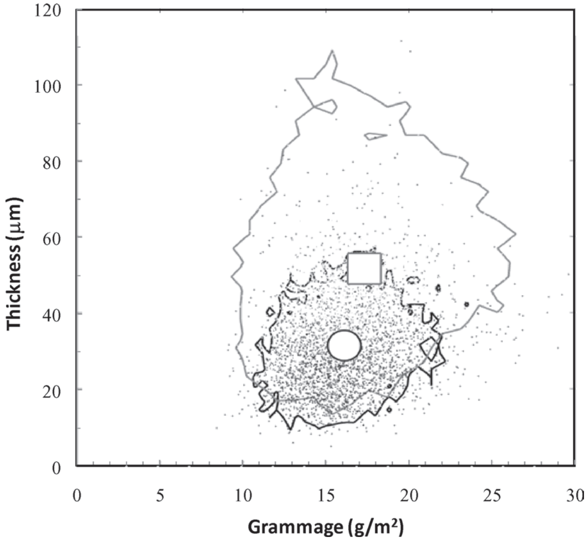

Figure 16. Distribution of thickness vs. grammage for sample N1. Contour lines indicate equal levels of constant population for the unpressed region (gray) extending to higher thickness values, and the pressed region (black) confined to lower thickness values. The symbols mark the mean value of the distributions; square – unpressed, circle – pressed.

thickness in one centimeter regions to a precision near that of fiber widths. The dimensions are ideal for characterizing induced structural features from the wet pressing (CWP) and through air drying (TAD) processes. The method is sensitive enough to measure creping patterns and distinguish between pleating and bulking of the web. As a noncontacting method, surface measurements are not subject to deformation under load that could produce erroneous results as the structure is changed.

Separation of thickness and out-of-plane deformation is important for characterizing the influence at a specific process or process variable has on the local structure. It is also essential for mapping the local density by the fusion of grammage maps with thickness maps. Local density is useful in characterizing the structure of the web, either as contacted fibers or for the investigation of structural porosity.

Spatial partitioning of the maps was introduced as a method for studying each of the structural features that combine to create the complex structure found in tissue and towel products. In this study, spatial partitioning based on either thickness or out-of-plane deformation was used to create image masks

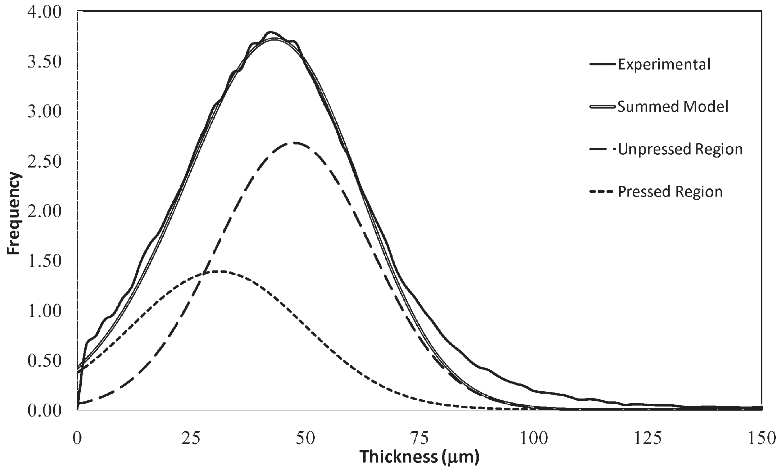

Figure 17. Frequency distribution of thickness values for sample N1. The experimental data is shown as the solid line. Two normal distributions were generated from the pressed (unmasked) and non-pressed (masked) partitions. The area under the distribution is a function of the spatial coverage of the specific masked region, centered at the mode. The pressed region is shown as a fine dashed line, while the unpressed region as coarse dashed line. The sum of the two model distributions is shown as the double line.

to isolate regions for separate analysis. Two paper towel samples were analyzed and compared. The sample (PT1) made by TAD showed an underlying relationship between thickness and grammage found in both the pressed and unpressed regions. A paper towel sample of lesser quality (PT3) showed out-of-plane deformation, but no indication of compression of the structure in the deformed features. The partitioning of the structure may be improved by using less subjective methods of defining regions; for example using embossing templates to generate images masks. It may also be useful to partition into more than two sections, to see how each contributes to the overall structure.

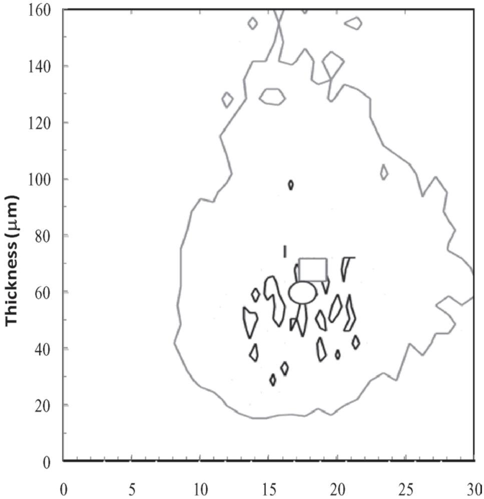

Figure 18. Distribution of thickness vs. grammage for sample TP1. Contour lines indicate equal levels of constant population for the unpressed region (gray) extending to higher thickness values, and the pressed region (black) confined to lower thickness values. The symbols mark the mean value of the distributions; square – unpressed, circle – pressed.

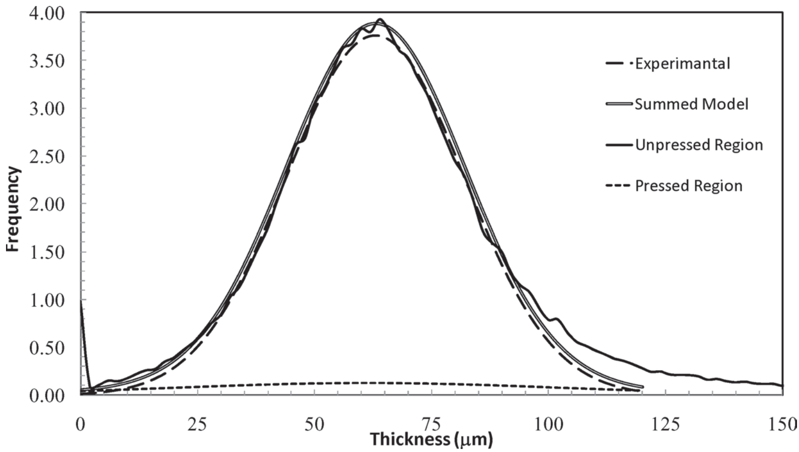

Figure 19. Frequency distribution of thickness values for sample TP1. The experimental data is shown as the solid line. Two normal distributions were generated from the partitioned distribution statistics, considering the spatial coverage of the masked region, and the mode of the distribution; pressed region – fine dashed line; unpressed region – coarse dashed line. The sum of the two model distributions is shown as the double line.

ACKNOWLEDGEMENTS

The authors gratefully acknowledge the financial support of the Research Foundation of the State of New York, Kimberly-Clark Corporation and the Shoupp Award from Miami University. . The helpful assistance of Dr. Robert Hanna and William Burry of SUNY-ESF, and Louis Troll (Undergraduate Summer Scholar) and Zachary McCoy of Miami University is also appreciated.

REFERENCES

1. Ramasubramanian, M. K., "Physical and Mechanical Properties of Towel and Tissue", in Handbook of Physical Testing of Paper, 2nd ed., ed. R.E. Mark, C.C. Haberger, J. Borch, and M.B. Lyne, Marcel Dekker, New York Vol 1:661–698, 2002.
2. Liang S. and Suhling, J. G., "Finite Element Modeling of the Embossing of Paper Sheets", in Products of Papermaking, Trans. 10th Fund.Res., The Pulp and Paper Fundamental Research Society, Bury, Lancashire, UK Vol 2:1073–1101, 1993.
3. TAPPI Standard Test Methods T410 om-02, "Grammage of Paper, Paperboard, and Combined Board. TAPPI, Atlanta, 2002.
4. TAPPI Standard Test Methods T411 om-05, "Thickness (Caliper) of Paper, Paperboard, and Combined Board. TAPPI, Atlanta, 2005.
5. Sung, Y-J., Ham, C. H, Kwon, O., Lee, H. L., and Keller, D. S. "Applications of Thickness and Apparent Density Mapping by Laser Profilometry", in Advances in Paper Science and Technology, Trans. 13th Fund. Res. Symp. Cambridge, UK, The Pulp and Paper Fundamental Research Society, Bury, Lancashire, UK Vol2:961–1007, 2005.
6. TAPPI Standard Test Methods T402 sp-05, "Standard conditioning and testing atmospheres for paper, board, pulp handsheets, and related products", TAPPI, Atlanta, 2005.
7. Keller, D. S. and Pawlak, J. J. "β-Radiographic imaging of paper formation using storage phosphor screens", J.Pulp Pap.Sci., **27**(4):117–123, 2001.
8. Keller, D. S., Kellomaki, M., Pawlak, J. J., Hagglund, J.-E., and Johansson, N. "Three Storage Phosphor Systems for β-radiographic Imaging of Paper", J.Pulp Pap.Sci., **19**(2):170–175, 2004.
9. Sung, Y.-J. "Influences of Consolidation Processes on Local Paper Structure", Ph.D. Dissertation, State Univeristy of New York, College of Environmental Science and Forestry, Syrcacuse, NY, USA 2002.
10. Fellers, C., Andersson, H., and Hollmark, H. "The Definition and Measurement of Thickness and Density" in Paper Structure and Properties, ed. J.A. Bristow and P. Kolseth. 151–1986, 1986.

11. Sung, Y.-J. and Keller, D. S. "Effects of Web Densification on the Structural Inhomogeneity of Paper", (abstract only) in Proceedings 2002 Progress in Paper Physics Seminar, Skaneateles, NY, SUNY College of ESF, Syracuse, NY. 163–167, 2002.

Transcription of Discussion

SPATIAL PARTITIONING OF THE STRUCTURAL PROPERTIES OF TISSUE AND TOWEL GRADES

D. S. Keller,[1,2] *D. Branca*[2] and *O. Kwon*[2]

[1]Department of Paper and Chemical Engineering, Miami University, Oxford, OH, USA, 45056
[2]Faculty of Paper Science and Engineering, SUNY College of Environmental Science and Forestry, Syracuse, New York, USA, 13210

Gary Baum PaperFuture Technologies

Thank you. My question is, did you separate the two plies that typically make up a paper towel when you did this? I noticed you had some that showed holes, which means you are looking at a single ply rather than both plies together.

Steve Keller

Thank you. That is a very good question. Forgive me for not mentioning that these are all single plies. The answer to your question is "Yes" in our next work where we have separated plies and tested them. They were all manufactured as single plies.

Gary Baum

Are you sure that "Bounty" is?

Steve Keller

There are many different types of "Bounty".

Discussion

Gary Baum

Yes, I have one right here, I have just separated it for you.

Steve Keller

We used "Bounty Basic". It is a single ply. When we started the project, we did not have a lot of money and then later on we bought the more expensive, 2-ply brands!

Matthias Schmitt Voith Paper Fabrics

What are your recommendation for tissue makers, or for us as a market leader for tissue fabrics? What is the conclusion, the added value out of your work?

Steve Keller

I have to acknowledge that I am unaware of what happens in tissue company technical centres. I have no idea how to provide you with an answer, because I have no idea what their questions are. The reason there is not a lot of literature regarding tissue and towel products is there is not a lot that has been spoken outside the four walls of those buildings. So, there may be specific questions that we get which are confidential to a specific company. I cannot really make any general points. I will say that we are pursuing things that are confidential, and also ones that are not proprietary, and so you will continue to see discoveries that are going to be useful, say, in a pre-competitive form.

It is difficult to say from our perspectives that this is going to improve things, as we would normally say for print quality, because all of that work is published widely. Whereas for specific tissue manufacturing processes, which are under confidentiality or intellectual property protection, we may not even know specific aspects of the processes. There are only a few general process methods that we know for these samples. Well I can say one thing; we are able to distinguish the differences between different product structures very clearly.

Matthias Schmitt

Just one additional question, do you see the possibility of connecting your work with absorbency?

Steve Keller

Yes, absolutely. That is why we are pursuing the current approach. That will be the next step, along with the mechanical properties and mechanical deformation.

Matthias Schmitt

Will we get something in four years with connection for us all to see?

Steve Keller

I hope so!

Stefan Lindström Mid Sweden University

You demonstrated that when you intentionally introduced two different types of area, by embossing for instance, you get the skewed distribution. Can you say the converse, that when you observe a skewed distribution, that implies that you have some particular structural feature in the paper?

Steve Keller

We are doing some work on hand sheets and printing papers now that tests reversibility of this method by inducing stochastic structures and blending them together to see if we can affect that grammage distribution in a similar way to what we have seen for towels. There are ways of changing the way a hand sheet is formed and then going back and seeing if that produces a skewed grammage distribution. We are working on it and I have nothing to report at this time.

Roger Gaudreault Cascades R&D

On the market there are tissue products which include lotions. Do you think that it is possible to connect your methods with analytical techniques to be able to detect or visualize where the chemistry is located?

Steve Keller

Not as the instrument is configured right now. Lotions present a chemical difference. When you consider wettability and absorbency, that is going to introduce another parameter. What we would like to do is to establish the mechanical, the spatial geometric structures first, and then take a look at the changes that are occurring with the surface chemistry. But to this note, the current method will not distinguish chemistry, although one could envision that if one were to do spectroscopy at each individual point, you may have something valuable. But I think we would have to have a finer resolution than the current instrument offers.